Three-Dimensional Transient Radiative Transfer Modeling Using Discontinuous Spectral Element Method

J.M. Zhao*[,1,2] and L.H. Liu[†, 1]

1. *Harbin Institute of Technology, Harbin 150001, People's Republic of China*

2. *The Hong Kong Polytechnic University, Hong Kong, People's Republic of China*

Nomenclature

a = Anisotropy parameter of linear anisotropic scattering phase function
A = Area, m^2
c = Speed of light, m/s
G = Integrated intensity defined by Eq. (8a), W/m^2
h = One-dimensional standard nodal basis function
$\hbar$ = Three-dimensional standard nodal basis function
$\mathbf{H}$ = Matrix defined in Eq. (7)
I = Radiative intensity, $W/(m^2sr)$
I_0 = Amplitude of transient intensity, $W/(m^2sr)$
I_b = Black body radiative intensity, $W/(m^2sr)$
I_p = Transient intensity on the boundary, $W/(m^2sr)$
$\mathbf{k}$ = Unit direction vector of *z*-direction
K = General hexahedral element
K_{st} = Standard hexahedral element
L_R = Reference length scale, m
M = Number of discrete ordinate directions
$\mathbf{M}$ = Matrix defined in Eq. (7)
$\mathbf{n}_w$ = Unit normal vector of the wall
$\mathbf{n}_{\partial K}$ = Unit normal vector at boundary of element K
N_t = Number of discretized time steps
N_{sk} = Number of solution nodes on each element
N_φ = Number of subdivisions for azimuthal angle
N_θ = Number of subdivisions for zenith angle
p = Order of polynomial expansion
q_z = Heat flux of z-direction defined by Eq. (8b), W/m^2
$\mathbf{r}$ = Vector of spatial coordinates, $\mathbf{r} = (x, y, z)$
t = Time, s
t^* = Dimensionless time $t^* = ct / L_R$, Dimensionless time step

*Ph.D, School of Energy Science and Engineering, 92 West Dazhi Street; jmzhaocn@gmail.com.
[†]Professor, School of Energy Science and Engineering, 92 West Dazhi Street; lhliu@hit.edu.cn, (corresponding author).

$\tilde{S}$ = Function defined in Eq. (7d), W/m^3
T = Temperature, K
u = Unit step function
V = Volume, m^3
w = Weight of discrete ordinates approximation, sr
x, y, z = Global coordinate system variables
$\mathbf{x}_{st}$ = Local coordinate vector, $\mathbf{x}_{st} = (x_{st}, y_{st}, z_{st})$
x_{st}, y_{st}, z_{st} = Reference coordinate system variables

Greek symbols
β = Extinction coefficient $\beta = (\kappa_a + \kappa_s)$, m^{-1}
$\tilde{\beta}$ = Function defined in Eq. (7c), m^{-1}
Δt^* = Dimensionless time step
θ = Zenith angle
κ_a = Absorption coefficient, scattering coefficient, m^{-1}
κ_s = Scattering coefficient, m^{-1}
ρ = Bidirectional reflection function
σ = Stefan-Boltzmann constant, W/(m^{2}K^4)
τ_L = Optical thickness, $\tau_L = \beta L$
τ_p = Transmissivity
ϕ = Global nodal basis function
φ = Azimuthal angle
Φ = Scattering phase function
ψ = Map function defined by Eq. (5)
ω = Single scattering albedo
$\mathbf{\Omega}$ = Unit vector of radiation direction
Ω = Solid angle, sr

Subscripts
n = Time step index
i = Mapped one-dimensional index
i', j', k' = Elemental spatial node index
l = Node index of standard hexahedral element
w = Value at wall

Superscripts
m, m' = Index of discrete ordinate direction

1. Introduction

Transient radiative transfer within a participating medium has attracted the interest of many researchers due to the availability of short pulse lasers and their application to many emerging new technologies [1-3]. A number of methods have been developed to solve the transient radiative transfer equation (TRTE), such as the Monte Carlo method [4], the integral equation method (IE) [5], the discrete ordinates method (DOM) [6, 7] and the finite volume method (FVM) [8]. Among them, the methods based on the differential form of

the TRTE, such as DOM, FVM, are efficient and easy to apply to problems with complex media and boundary conditions. However, the DOM and the FVM suffer from large false scattering, and the transient wave front cannot be captured efficiently and accurately.

Recently, based on a discontinuous Galerkin (DG) approach, Liu and Hsu [9] developed and analyzed transient radiative transfer in two-dimensional graded index media using a discontinuous finite element method (DFEM). In the DG approach, the approximation space is composed of discontinuous functions, which is expected to be ideal in solving transient radiative transfer problems and accurately capturing the sharp wave fronts. The DFEM showed good performance in solving the transient radiative transfer problems. As an advanced version of the DFEM, a discontinuous spectral element method (DSEM) [10], which enriches the DFEM due to the high order accuracy of the spectral method, was developed to solve transient radiative transfer problems. The DSEM was shown to be efficient and accurate in capturing the sharp wave front of the transient radiative transfer process. However, performance of the DSEM has only been examined in one- and two- dimensional cases.

In this note, the DSEM is formulated and applied to solve the three-dimensional transient radiative transfer problems. Its performance in solving three-dimensional transient radiative transfer is studied and verified.

2. Transient Radiative Transfer Equation

The discrete-ordinates form of the TRTE for an absorbing, nonemitting and scattering medium can be written as [11]

$$\frac{\partial I^m(\mathbf{r},t)}{c\,\partial t} + \mathbf{\Omega}^m \bullet \nabla I^m(\mathbf{r},t) + \beta I^m(\mathbf{r},t) = \frac{\kappa_s}{4\pi}\sum_{m'=1}^{M} I^{m'}(\mathbf{r})\,\Phi(\mathbf{\Omega}^m,\mathbf{\Omega}^{m'})\,w^{m'}, \tag{1a}$$

with the boundary condition and initial condition given as [11]

$$I^m(\mathbf{r}_w,t) = I_p(\mathbf{r}_w,\mathbf{\Omega}^m,t)\tau_p(\mathbf{r}_w,\mathbf{\Omega}^m) + \sum_{\mathbf{n}_w\bullet\mathbf{\Omega}^{m'}<0} \rho(\mathbf{r}_w,\mathbf{\Omega}^m,\mathbf{\Omega}^{m'}) I_w^{m'} \left|\mathbf{n}_w\bullet\mathbf{\Omega}^{m'}\right| w^{m'},\ \ \mathbf{n}_w\bullet\mathbf{\Omega}<0, \tag{1b}$$

$$I(\mathbf{r},\mathbf{\Omega},t) = 0, \qquad t = 0. \tag{1c}$$

The DSEM is then developed based on Eqs. (1) to model transient radiative transfer processes.

3. DSEM Discretization

The radiative intensity field of the *n*th time step and direction $\mathbf{\Omega}^m$ is approximated in a function space

spanned by Chebyshev nodal basis functions defined on an element K as [10]

$$I_n^m(\mathbf{r}) \simeq \sum_{i=1}^{N_{sk}} I_{n;i}^m \phi_i(\mathbf{r}) \tag{2}$$

where $I_{n;i}^m$ denotes the radiative intensity of the *i*th node, and ϕ_i is the nodal basis function of node *i* defined on K. In the present study, the solution domain is subdivided into hexahedral elements. The standard element K_{st}, defined in the reference coordinate system as shown in Fig. 1, is a cube: $K_{st}: x_{st}, y_{st}, z_{st} \in [-1,1]$. The three-dimensional nodal basis function defined on K_{st} is formulated as

$$\hbar_i(x_{st}, y_{st}, z_{st}) = h_{i'}(x_{st}) h_{j'}(y_{st}) h_{k'}(z_{st}), \quad i', j', k' = 1, ..., p+1, \quad i = 1, ..., (p+1)^3 \tag{3}$$

where, $h_{i'}$ is the one-dimensional Chebyshev nodal basis function defined on [-1,1] [12], and i is an index map defined as $i = i(i', j', k') = i' + (j'-1)(p+1) + (k'-1)(p+1)$, here p is the order of Chebyshev polynomial expansion.

The elemental nodal basis function $\phi_i(x, y, z)$ defined on a general hexahedron element K can be obtained from the reference basis function $\hbar_i(x_{st}, y_{st}, z_{st})$ defined on standard element K_{st} using a coordinate transformation as depicted in Fig. 1. The coordinate transformation is defined based on the coordinates of the eight vertices of K_{st} ($\mathbf{x}_{st,l}$, $l = 1, ..., 8$) as shown in Fig. 1, and the corresponding coordinates of the eight vertices of K, $\mathbf{r}_l$, as

$$\mathbf{r}(\mathbf{x}_{st}) = \sum_{l=1}^{8} \mathbf{r}_l \psi_l(\mathbf{x}_{st}), \quad \mathbf{r} = (x, y, z) \in K, \quad \mathbf{x}_{st} = (x_{st}, y_{st}, z_{st}) \in K_{st} \tag{4}$$

where ψ_l is a mapping function related to the vertex $\mathbf{x}_{st,l}$, which is defined as

$$\psi_l(\mathbf{x}_{st}) = \frac{1}{8}\left[1 + \mathrm{sign}(x_{st,l}) x_{st}\right]\left[1 + \mathrm{sign}(y_{st,l}) y_{st}\right]\left[1 + \mathrm{sign}(z_{st,l}) z_{st}\right], \quad l = 1, ..., 8 \tag{5}$$

Then $\phi_i(x, y, z)$ is obtained from $\hbar_i(x_{st}, y_{st}, z_{st})$ as

$$\phi_i[\mathbf{r}(\mathbf{x}_{st})] = \hbar_i(\mathbf{x}_{st}) \tag{6}$$

By substituting the three-dimensional spectral approximation of the intensity field [Eq. (2)] into the TRTE [Eq. (1)] and following the general discontinuous Galerkin approach outlined in preceding work [10, 13], the final DSEM discretization of Eq. (1) over element K at the *n*th time step is obtained as

$$\mathbf{M}_n^m \mathbf{I}_n^m = \mathbf{H}_n^m, \qquad n = 1, ..., N_t \tag{7a}$$

where the matrices $\mathbf{M}_n^m$ and $\mathbf{H}_n^m$ are defined respectively as

$$M_{n;\,ji}^{m} = -\int_K \phi_i \, \mathbf{\Omega}^m \bullet \nabla \phi_j \mathrm{d}V + \frac{1}{2}\int_{\partial K} \left(\mathbf{\Omega}^m \bullet \mathbf{n}_{\partial K} + \left| \mathbf{\Omega}^m \right| \right) \phi_i \, \phi_j \mathrm{d}A + \int_K \tilde{\beta}_n \, \phi_i \, \phi_j \mathrm{d}V \,, \tag{7b}$$

$$H_{n;\,j}^{m} = \int_K \tilde{S}_n^m \, \phi_j \mathrm{d}V - \frac{1}{2}\int_{\partial K} \left(\mathbf{\Omega}^m \bullet \mathbf{n}_{\partial K} - \left| \mathbf{\Omega}^m \right| \right) I_n^{m,-} \phi_j \mathrm{d}A \,, \tag{7c}$$

where the superscript operator "-" denote the values at the outside of element K [10], in which $\tilde{\beta}_n$ and $\tilde{S}_n(\mathbf{r}, \mathbf{\Omega})$ are defined respectively as

$$\tilde{\beta}_n = \frac{2}{L_R \Delta t^*} + \beta \,, \tag{7d}$$

$$\begin{aligned} \tilde{S}_n^m(\mathbf{r}) = {} & \frac{\kappa_s}{4\pi} \sum_{m'=1}^{M} \left[I_n^{m'}(\mathbf{r}) + I_{n-1}^{m'}(\mathbf{r}) \right] \Phi(\mathbf{\Omega}^m, \mathbf{\Omega}^{m'}) \, w^{m'} \\ & - \mathbf{\Omega}^m \bullet \nabla I_{n-1}^m(\mathbf{r}) - \left[\beta - \frac{2}{L_R \Delta t^*} \right] I_{n-1}^m(\mathbf{r}) \end{aligned} \,, \tag{7e}$$

where L_R is a reference length and is selected as the characteristic length of the problem, $t^* = ct / L_R$ is dimensionless time and Δt^* is the dimensionless time step. The matrix equations given by Eqs. (7) are solved element by element at each time step through Gaussian elimination.

4. Results and Discussion

The DSEM described above is applied to solve the transient radiative transfer problem in a cubic medium of side length *L* for the boundary-driven problems listed in Table 1. As for numerical solution, the cubic medium is defined in the global coordinate system (Fig. 1) with $x, y, z \in [0, L]$, which will thereafter be subdivided into many small rectangular hexahedral elements as described in Section 3 during the DSEM solution. The medium is initially cold. In the first case, diffuse radiation is emitted from the bottom wall ($z = 0$) of the cube at $t = 0$ and then travels in the medium at a finite speed c. At any given time t, the wave front will travels a distance $z = ct$, hence the dimensionless time $t^* = ct / L = z / L$ gives the exact fractional position of the wave front.

The transient incident radiation function (or integrated intensity) $G(x, y, z, t)$ and the z-direction transient radiative heat flux $q_z(x, y, z, t)$ distribution along the centerline of the cube ($x = 0, y = 0$)

obtained by DSEM for Case 1 are presented in Figs. 2 (a) and (b), respectively. The transient incident radiation function and radiative heat flux of z-direction is defined and computed as

$$G(x,y,z,t)=\int_0^{2\pi}\int_0^{\pi} I(x,y,z,t,\theta,\varphi)\sin\theta \mathrm{d}\theta \mathrm{d}\varphi \tag{8a}$$

$$q_z(x,y,z,t)=\int_0^{2\pi}\int_0^{\pi} I(x,y,z,t,\theta,\varphi)\cos\theta\sin\theta \mathrm{d}\theta \mathrm{d}\varphi \tag{8b}$$

The results obtained using the YIX method [14] are also shown as a comparison. Here, two mesh decomposition schemes are used for the DSEM, namely, $N_x\times N_y\times N_z=2\times2\times17$ elements with $p=1$ and $N_x\times N_y\times N_z=1\times1\times17$ elements with $p=2$, where N_x, N_y and N_z denote the number of elements (subdivisions) for corresponding dimensions. These two spatial decompositions require comparable computational effort. The angular discretization uses the S_N approximation [15]. The direct component of diffuse irradiation is discretized into $N_\theta\times N_\varphi=60\times120$ equivalent beams by a PCA scheme following the special treatment described in Ref. 10. For the temporal discretization, the dimensionless time step is taken as $\Delta t^*=1/34$. The typical computation time for this case by a Pentium 4 1.8 Ghz computer is about 30 minutes. Generally, for different instants in time, the results of the DSEM agree very well with the results of the YIX method [14]. The maximum relative error based on the results of YIX method is less than 3%. It is seen that the higher order approximation ($p=2$) gives better accuracy. Because the DSEM allows discontinuities at the element boundary, it ensures accurate prediction of the wave front when it is located on the element boundary. This characteristic of the DSEM agrees well with the examination conducted in one and two dimensions [10].

In the second case, the DSEM is applied to model transient radiative transfer in an anisotropically scattering medium. The scattering phase function of the medium is $\Phi(\mathbf{\Omega},\mathbf{\Omega}')=1+a\mathbf{\Omega}\bullet\mathbf{\Omega}'$. For a = -1, 0 and 1, the phase function is backward, isotropic and forward scattering, respectively. The transient incident radiation and the radiative heat flux distribution along the centerline of the cube ($x=0, y=0$) obtained by the DSEM for Case 2 are shown in Figs. 3 (a) and (b), respectively. The cube is decomposed into $N_x\times N_y\times N_z=2\times2\times17$ elements with $p=2$ for the spectral element approximation. The angular discretization is by the S_6 approximation. The direct component of diffuse irradiation is discretized

into $N_\theta \times N_\varphi = 160 \times 80$ equivalent beams by the PCA scheme. The DSEM accurately predicts the wave front at different instants of time. Compared to isotropic scattering, forward scattering significantly enhances heat flux, which is the opposite for backward scattering. This is reasonable because more energy emitted from the bottom wall is scattered upward (in the positive *z*-direction) for forward scattering, and vice versa for backward scattering. The effect of different phase functions on the incident radiation results in more complex behavior. At a given instant in time, both enhancement and weakening happens in the incident radiation curve.

A collimated beam propagating through a purely isotropic scattering medium of three different optical thicknesses, namely, $\tau_L =$ 0.1, 1 and 2, is considered in the third case. The beam enters the bottom wall of the cube and transmits in the *z*-direction. The transient incident radiation and the radiative heat flux distribution along the centerline of the cube ($x = 0, y = 0$) obtained by the DSEM for Case 3 are shown in Figs. 4 (a) and (b), respectively. In this study, the cube is divided into $N_x \times N_y \times N_z = 4 \times 4 \times 10$ elements with $p = 2$ for the spectral element approximation. The angular discretization uses the S_8 approximation. The dimensionless time step is taken as $\Delta t^* = 0.02$. Here, the dimensionless time t^* gives the position of the wave front as was the situation for the former cases. The DSEM accurately predicts the transient sharp wave fronts for different instants in time. With increasing optical thickness, the scattering effect is enhanced. A peak appears in the incident radiation curve at each instant in time. The position of maximum incident radiation is not at the bottom wall, which is due to the scattering contribution. At each instant in time, the heat flux distribution monotonically decreases with increasing optical thickness. The DSEM shows very good performance in solving a transient collimated beam radiative transfer problem and can accurately capture the sharp wave fronts.

5. Conclusions

A discontinuous spectral element method (DSEM) is presented to solve transient radiative transfer problems in a three-dimensional semitransparent medium. The performance of the DSEM in modeling three-dimensional transient radiative transfer processes is examined. The predictions of the DSEM agree well with reported solutions in the literature. The DSEM is demonstrated to be efficient and accurate in capturing the sharp wave fronts of a transient radiative transfer process. Because of high accuracy of

spatial discretization, accurate results can be obtained by DSEM with relatively few elements.

Acknowledgements

The authors thank Prof. Ronald L. Dougherty for his carefully reading and warmhearted help in improving the English text and the quality of the paper. The support of this work by the National Nature Science Foundation of China (50636010, 50425619) is gratefully acknowledged.

References

[1] Kumar, S. and Mitra, K., "Microscale Aspects of Thermal Radiation Transport and Laser Application," *Advances in Heat Transfer*, Vol. 33, 1999, pp. 187-294.

[2] Yamada, Y., "Light-Tissue Interaction and Optical Imaging in Biomedicine," *Annual Review of Heat Transfer*, Vol. 6, No. 6, 1995, pp. 1-59.

[3] Nussbaum, E. L., Baxter, G. D. and Lilge, L., "A Review of Laser Technology and Light-Tissue Interactions as a Background to Therapeutic Applications of Low Intensity Lasers and Other Light Sources," *Physical Therapy Reviews*, Vol. 8, No. 1, 2003, pp. 31-44.

[4] Guo, Z., Kumar, S. and San, K., "Multidimensional Monte Carlo Simulation of Short-Pulse Laser Transport in Scattering Media," *JTHT*, Vol. 14, No. 4, 2000, pp. 504-511.

[5] Tan, Z. M. and Hsu, P. F., "An Integral Formulation of Transient Radiative Transfer," *ASME Journal of Heat Transfer*, Vol. 123, No. 3, 2001, pp. 466-475.

[6] Guo, Z. and Kumar, S., "Discrete-Ordinates Solution of Short-Pulsed Laser Transport in Two-Dimensional Turbid Media," *Applied Optics*, Vol. 40, No. 19, 2001, pp. 3156-3163.

[7] Mitra, K., Lai, M.-S. and Kumar, S., "Transient Radiation Transport in Participating Media with a Rectangular Enclosure," *JTHT*, Vol. 11, No. 3, 1997, pp. 409-414.

[8] Chai, J. C., "One-Dimensional Transient Radiation Heat Transfer Modeling Using a Finite-Volume Method," *Numerical Heat Transfer Part B*, Vol. 44, No. 2, 2003, pp. 187-208.

[9] Liu, L. H. and Hsu, P.-f., "Analysis of Transient Radiative Transfer in Semitransparent Graded Index Medium," *Journal of Quantitative Spectroscopy and Radiative Transfer*, Vol. 105, No. 3, 2007, pp. 357-376.

[10] Zhao, J. M. and Liu, L. H., "Discontinuous Spectral Element Approach for Solving Transient Radiative Transfer Equations," *JTHT*, Vol. 22, No. 1, 2008, pp. 20-28.

[11] Liu, L. H. and Hsu, P.-f., "Time Shift and Superposition Method for Solving Transient Radiative Transfer Equation," *Journal of Quantitative Spectroscopy & Radiative Transfer*, Vol. 109, 2008, pp. 1297-1308.

[12] Zhao, J. M. and Liu, L. H., "Least-Squares Spectral Element Method for Radiative Heat Transfer in Semitransparent Media," *Numerical Heat Transfer Part B*, Vol. 50, No. 5, 2006, pp. 473-489.

[13] Zhao, J. M. and Liu, L. H., "Discontinuous Spectral Element Method for Solving Radiative Heat Transfer in Multidimensional Semitransparent Media," *Journal of Quantitative Spectroscopy and Radiative Transfer*, Vol. 107, No. 1, 2007, pp. 1-16.

[14] Tan, Z.-M. and Hsu, P.-f., "Transient Radiative Transfer in Three-Dimensional Homogeneous and Nonhomogeneous Participating Media," *Journal of Quantitative Spectroscopy and Radiative Transfer*, Vol. 73, Nos. 2-5, 2002, pp. 181-194.

[15] Fiveland, W. A., "Discrete-Ordinates Solution of the Radiative Transport Equation for Rectangular Enclosures," *ASME Journal of Heat Transfer*, Vol. 106, 1984, pp. 699-706.

Table 1. Boundary condition and medium property for different cases.

Case	Bottom boundary ($z = 0$)	Medium property	Other boundaries
1	diffuse emission, $I_p = I_0 u(t),\ I_0 = 1\ \mathrm{W/m^2 sr}$	isotropic scattering, $\tau_L = 1,\ \ \omega = 0.1$	transparent, non-reflective
2	diffuse emission, $I_p = I_0 u(t),\ I_0 = 1\ \mathrm{W/m^2 sr}$	linear anisotropic scattering: $\Phi = 1 + a\mathbf{\Omega}\bullet\mathbf{\Omega}'$ $\tau_L = 1, \omega = 1, a = -1, 0, 1$	transparent, non-reflective
3	Collimated intensity in z-direction, $I_p = I_0 u(t)\delta(\mathbf{\Omega} - \mathbf{k}),\ I_0 = 1\ \mathrm{W/m^2 sr}$	isotropic scattering, $\tau_L = 0.1, 1, 2,\ \ \omega = 1$	transparent, non-reflective

*note: here $u(t)$ is the unit step function, which is unity for $t > 0$, and zero otherwise. $\mathbf{k}$ is the unit direction vector of the z-direction.

Figure Captions

Figure 1. Schematic of coordinate transformation from a cubic standard element K_{st} defined in the reference coordinate system (x_{st}, y_{st}, z_{st}) to a general hexahedral element K in the global coordinate system (x, y, z).

Figure 2. Transient incident radiation function and heat flux distribution along the centerline of a cube with one diffusive emission boundary: **(a)** incident radiation function, **(b)** heat flux.

Figure 3. Transient incident radiation function and heat flux distribution along the centerline of a cube filled with linear anisotropic scattering medium: **(a)** incident radiation function, **(b)** heat flux.

Figure 4. Transient incident radiation function and heat flux distribution along the centerline of a cube with one collimated intensity emitting boundary: **(a)** incident radiation function, **(b)** heat flux.

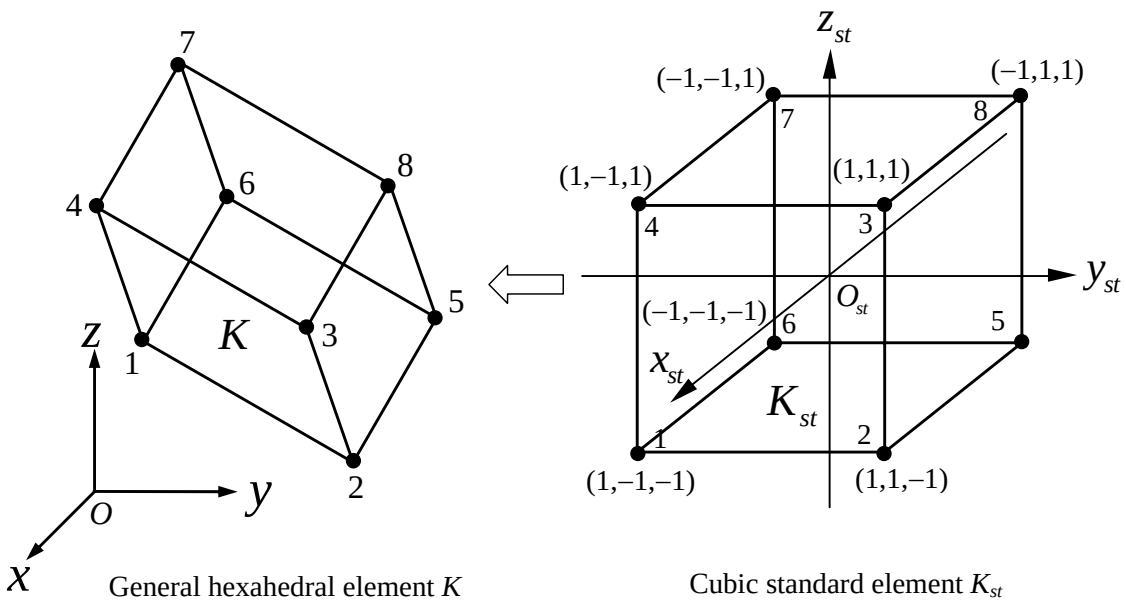

Figure 1

Authors: Zhao and Liu

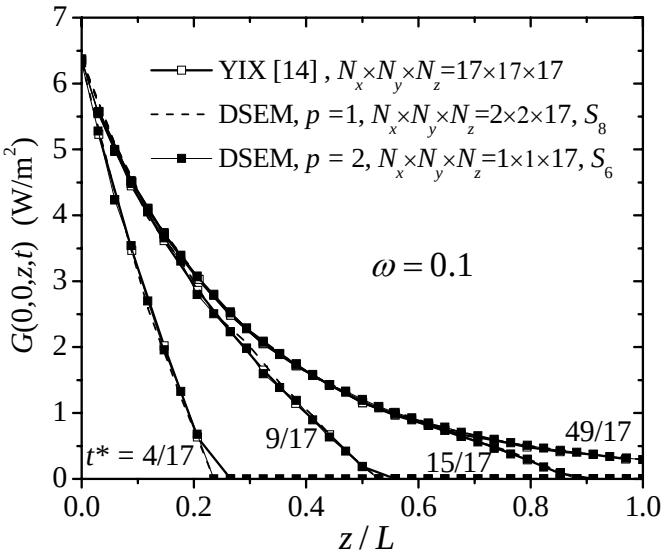

Figure 2 (a)

Authors: Zhao and Liu

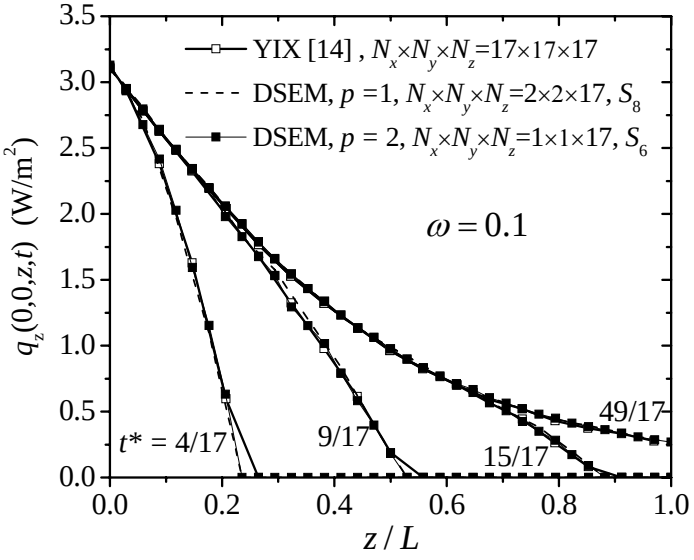

Figure 2 (b)

Authors: Zhao and Liu

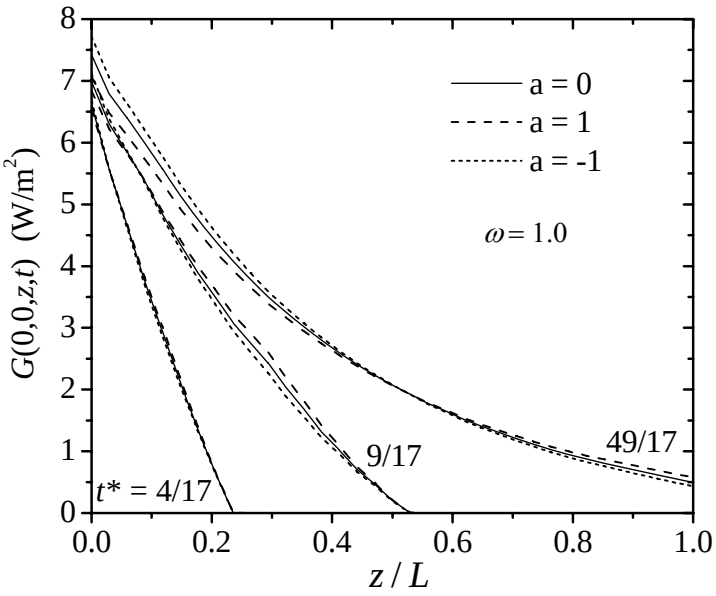

Figure 3 (a)

Authors: Zhao and Liu

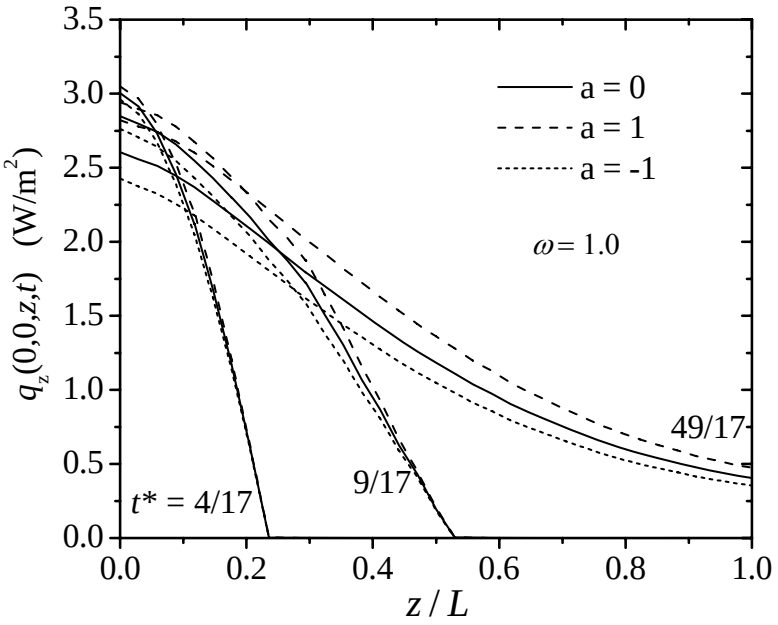

Figure 3 (b)

Authors: Zhao and Liu

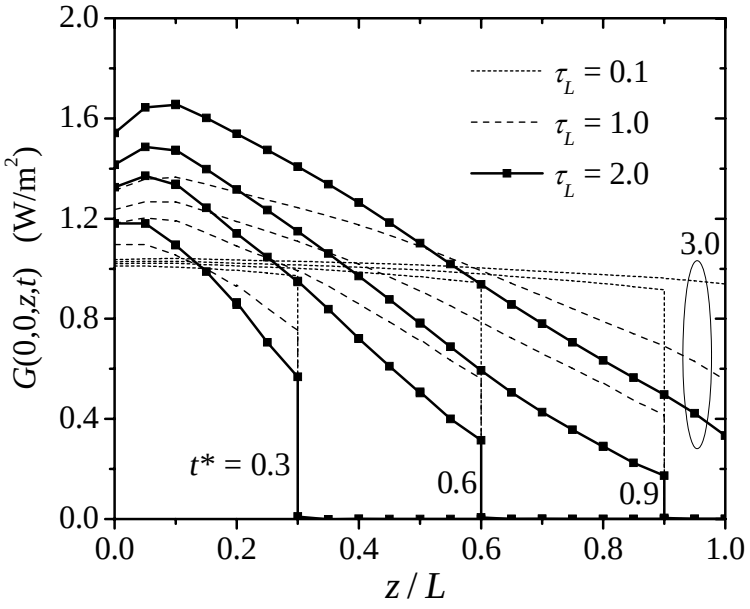

Figure 4 (a)

Authors: Zhao and Liu

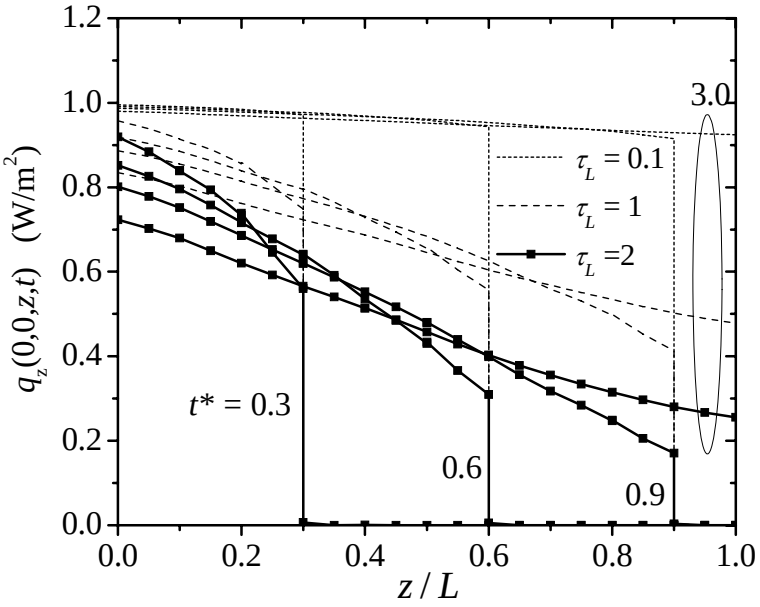

Figure 4 (b)

Authors: Zhao and Liu